Supplementary Information
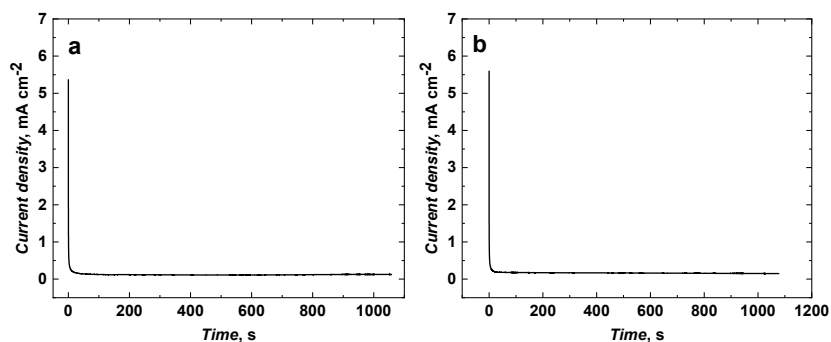
# Tailoring of the poly[Ni(OH)$_2$Salen] nanoparticles-based electrocatalysts for effective urea remediation

Monika Mierzejewska, Kamila Łępicka*, Jakub Kalecki, and Piyush Sindhu Sharma*

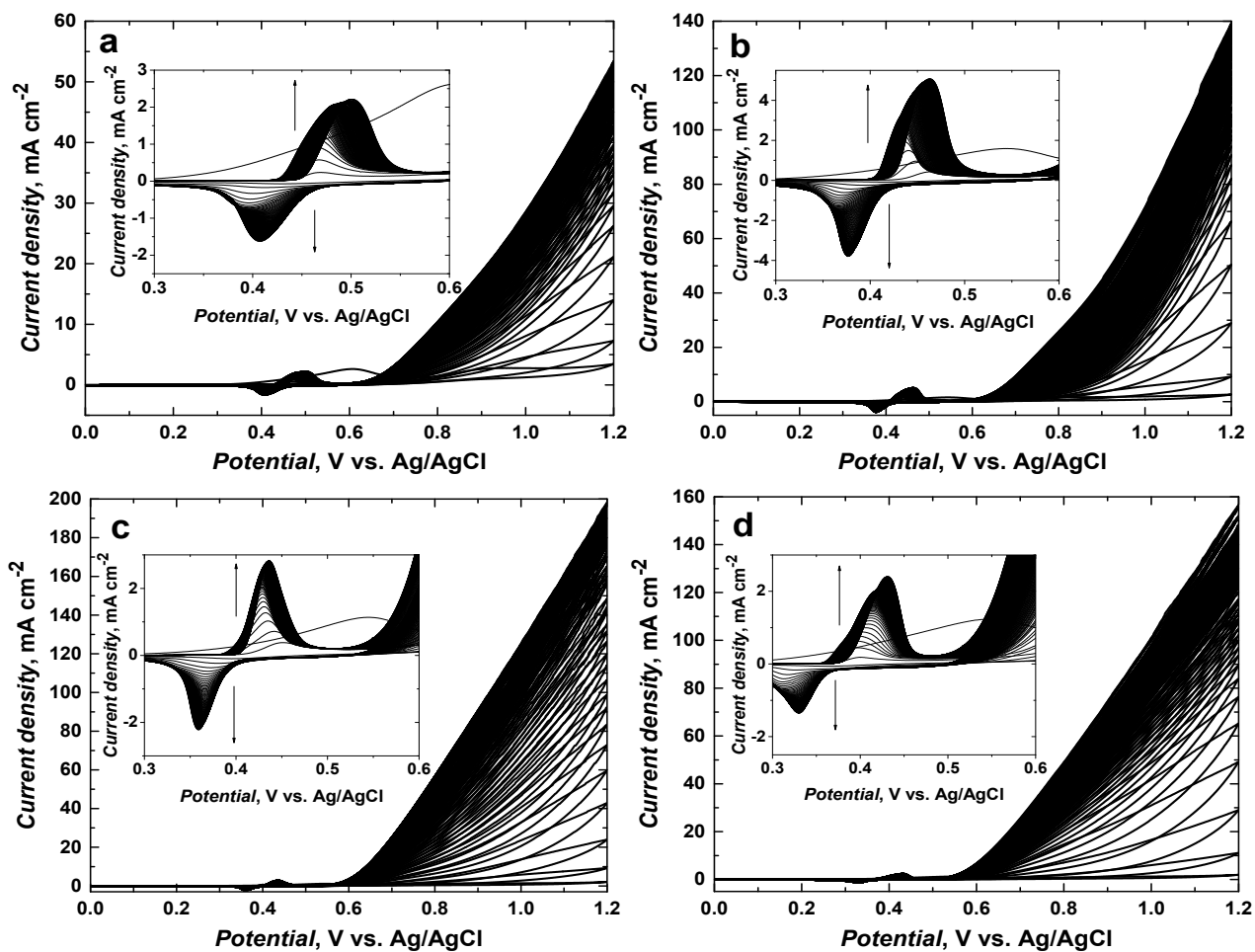Institute of Physical Chemistry, Polish Academy of Sciences, Kasprzaka 44/52, 01-224 Warsaw,

Poland

Figure S1. Potentiostatic depositions of (a) poly(NiSaltMe)$_{130}$ and (b) poly(*meso*-NiSaldMe)$_{130}$.
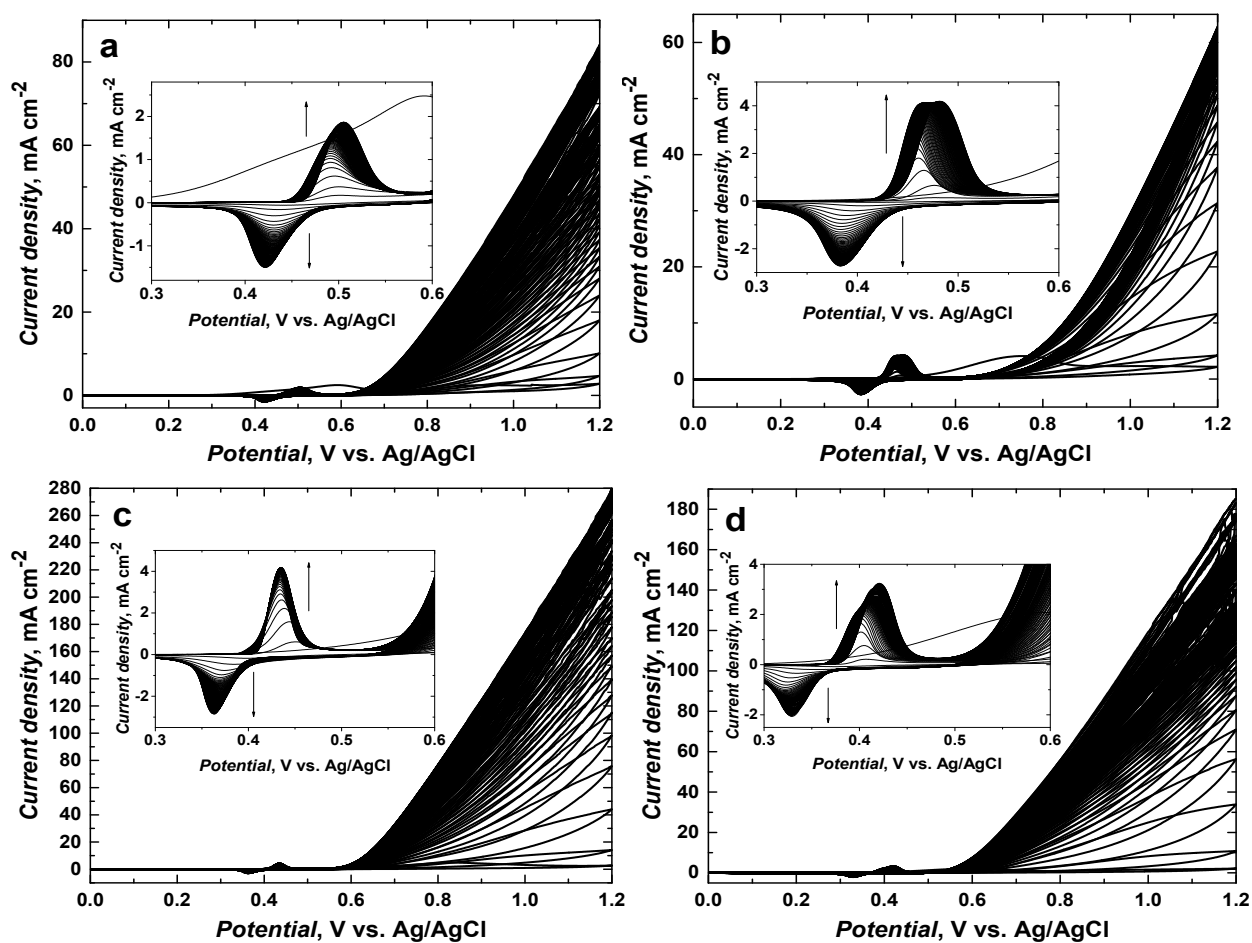
Figure S2. Multi-cyclic curves of potential driven NPs generation from poly(NiSaltMe)$_{130}$ performed in (a) 0.2 M NaOH$_{aq}$, (b) 0.5 M NaOH$_{aq}$, (c) 1.0 M NaOH$_{aq}$ and (d) 2.0 M NaOH$_{aq}$ at 20 mV s^{-1}.

2

Figure S3. Multi-cyclic curves of potential driven NPs generation from poly(*meso*-NiSaldMe)$_{130}$ performed in (a) 0.2 M NaOH$_{aq}$, (b) 0.5 M NaOH$_{aq}$, (c) 1.0 M NaOH$_{aq}$ and (d) 2.0 M NaOH$_{aq}$ at 20 mV s^{-1}.
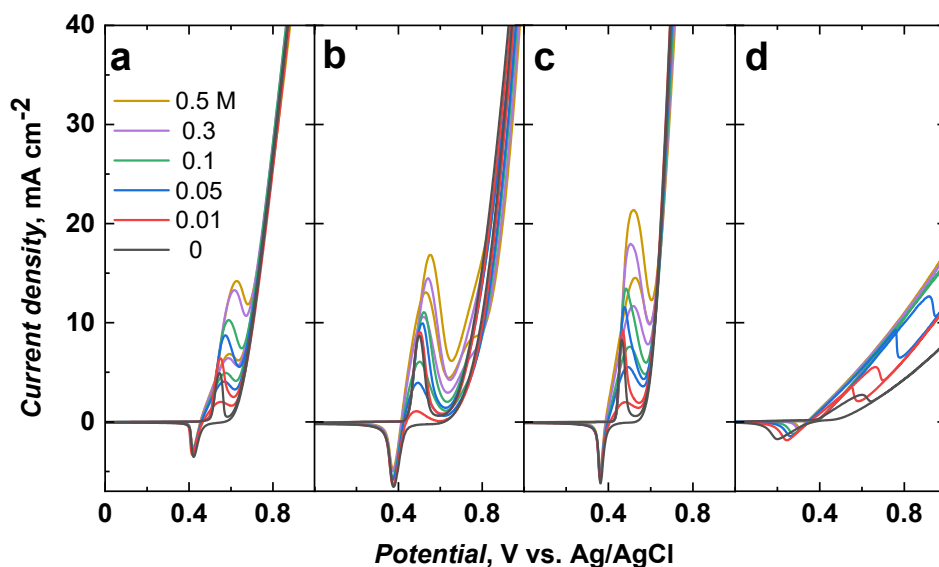
Figure S4. The catalytic CV responses of Ni(OH)$_2$-type NPs derived from poly(NiSaltMe)$_{130}$ towards various urea concentrations. Urea was added continuously in electrochemical cell after each electrocatalysis step to reach desired concentration. The CVs were performed at 50 mV s^{-1} in (a) 0.2 M NaOH$_{aq}$, (b) 0.5 M NaOH$_{aq}$, (c) 1.0 M NaOH$_{aq}$ and (d) 2.0 M NaOH$_{aq}$.
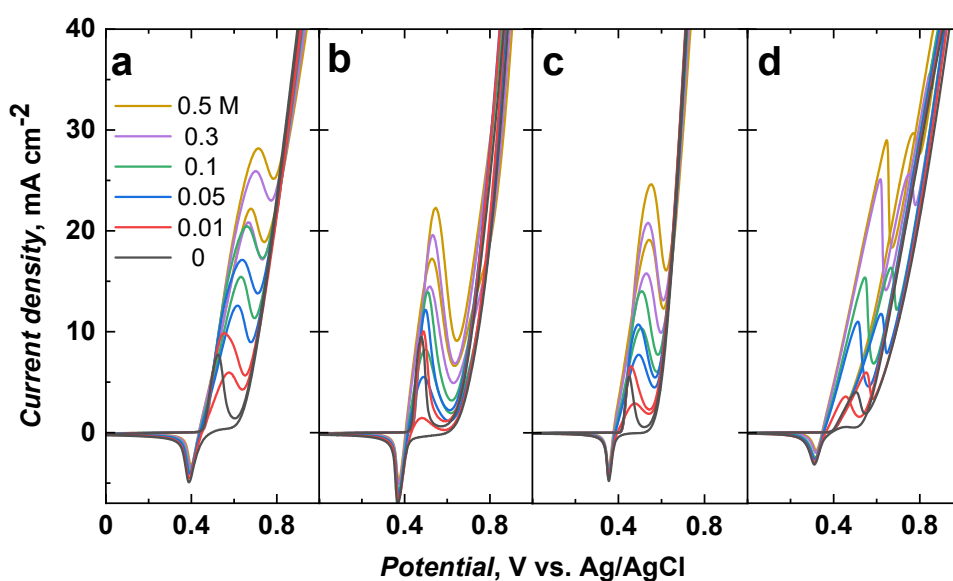
**Figure S5**. The catalytic CV responses of Ni(OH)$_2$ type NPs derived from poly(*meso*-NiSaldMe)$_{130}$, towards various concentrations of urea. Urea was added continuously in electrochemical cell after each electrocatalysis step to reach desired concentration. The CVs were performed at 50 mV s^{-1} in (a) 0.2 M NaOH$_{aq}$, (b) 0.5 M NaOH$_{aq}$, (c) 1.0 M NaOH$_{aq}$ and (d) 2.0 M NaOH$_{aq}$.
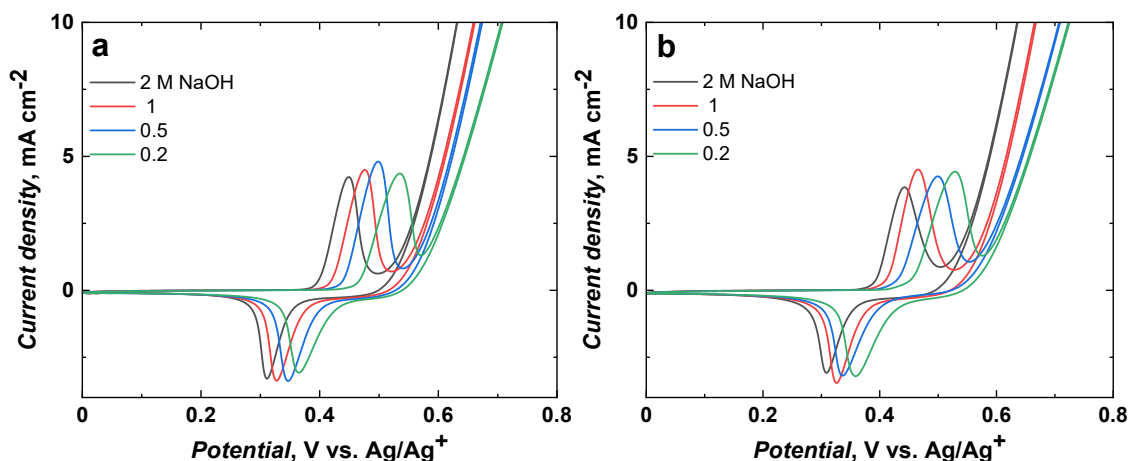
Figure S6. The CV responses of (a) poly[NPs-Ni(OH)$_2$SaltMe]$_{1\,M}$, (b) poly[*meso*-NPs-Ni(OH)$_2$SaldMe]$_{1\,M}$ in various NaOH$_{aq}$ concentrations. The CVs were performed at 50 mV s^{-1}.
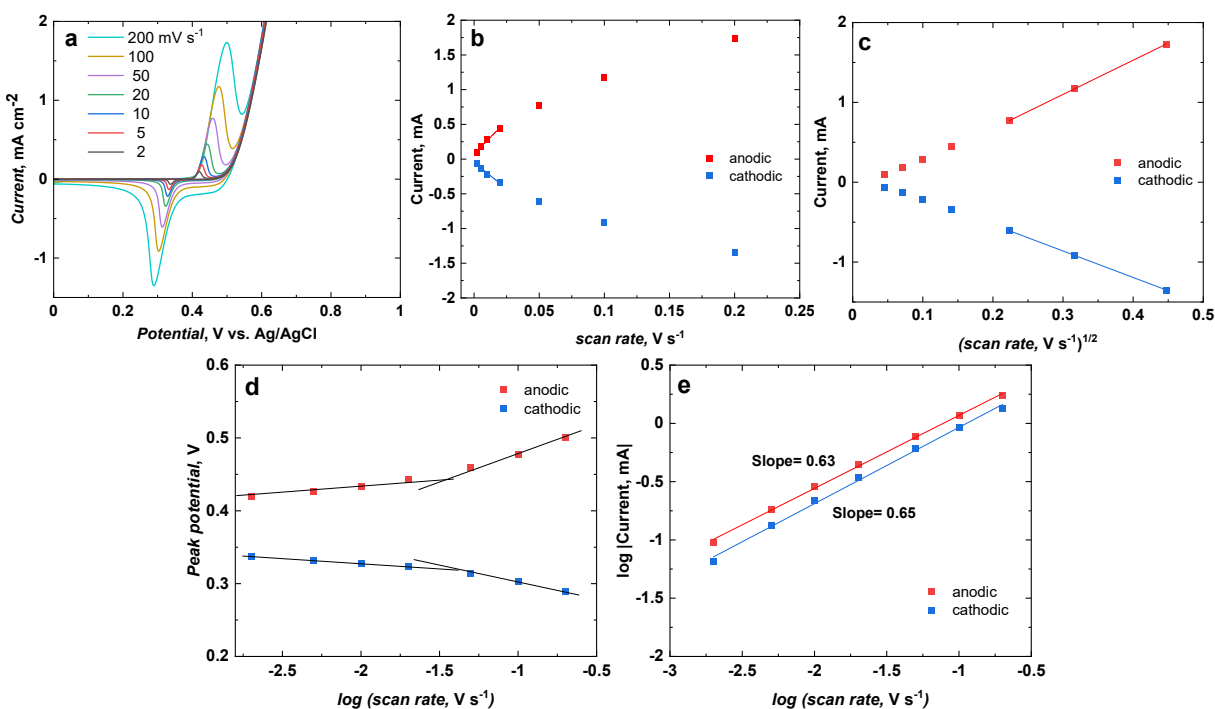
Figure S7. (a) CV curves of poly[NPs-Ni(OH)$_2$SaltMe]$_{1\,M}$ performed at 2, 5, 10, 30, 50, 100, 200 mV s^{-1} scan rate in 2.0 M NaOH$_{aq}$. (b) The anodic (red curve) and cathodic (blue curve) peak current dependence on the scan rate. (c) The anodic and cathodic peak currents vs. the square root of the scan rate. (d) The anodic and cathodic peak potentials vs. the logarithm of the scan rate. (e) The logarithm of the anodic and cathodic peak currents vs. the logarithm of the scan rate.

5
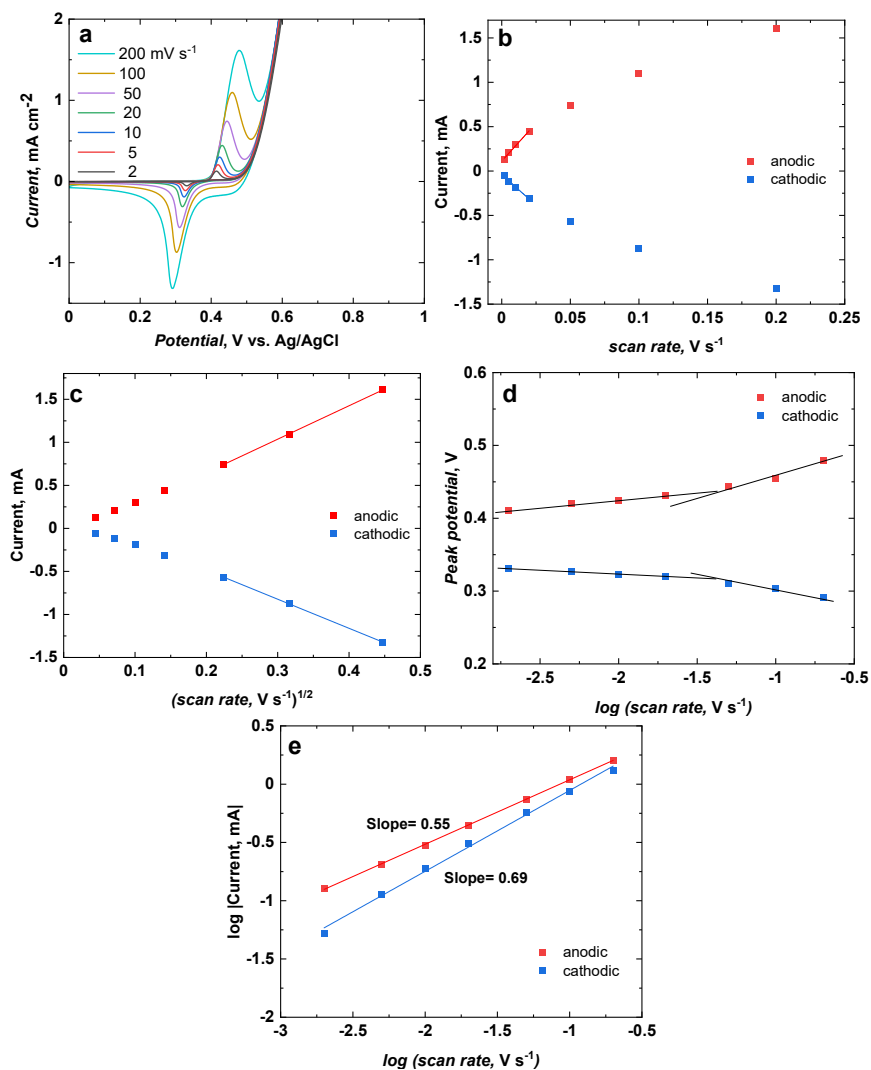
Figure S8. (a) CV curves of poly[*meso*-NPs-Ni(OH)$_2$SaldMe]$_{1\,M}$ at 2, 5, 10, 30, 50, 100, 200 mV s^{-1} scan rate in 2.0 M NaOH$_{aq}$ (b) The anodic (red curve) and cathodic (blue curve) peak current dependence on the scan rate. (c) The anodic and cathodic peak currents vs. the square root of the scan rate. (d) The anodic and cathodic peak potentials vs. the logarithm of the scan rate. (e) The logarithm of the anodic and cathodic peak currents vs. the logarithm of the scan rate.
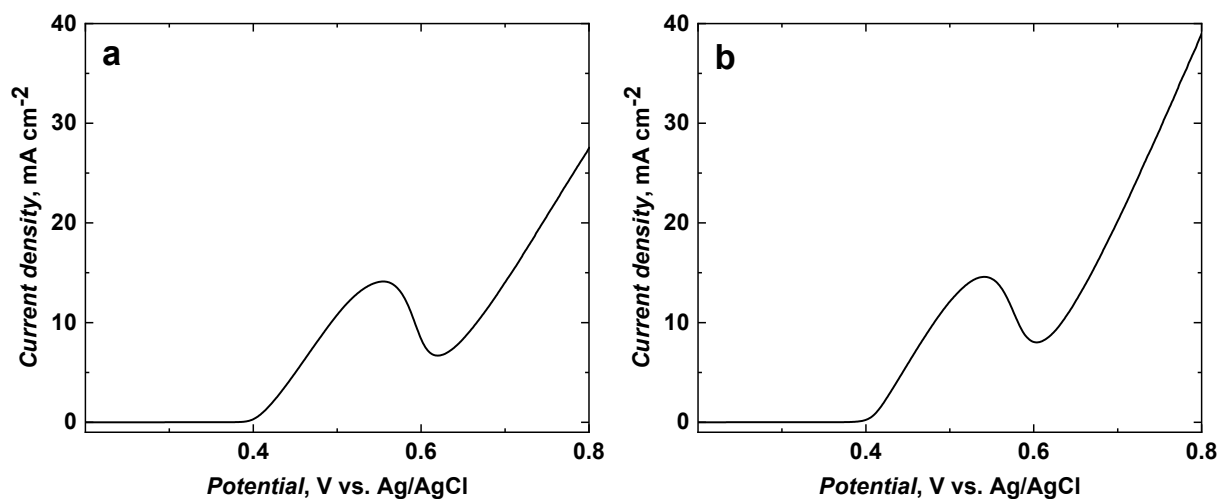
Figure S9. LSV curves of (a) poly[NPs-Ni(OH)$_2$SaltMe]$_{1\,M}$ and (b) poly[*meso*-NPs-Ni(OH)$_2$SaldMe]$_{1\,M}$ registered with the scan rate of 5 mV s^{-1} in different solutions.
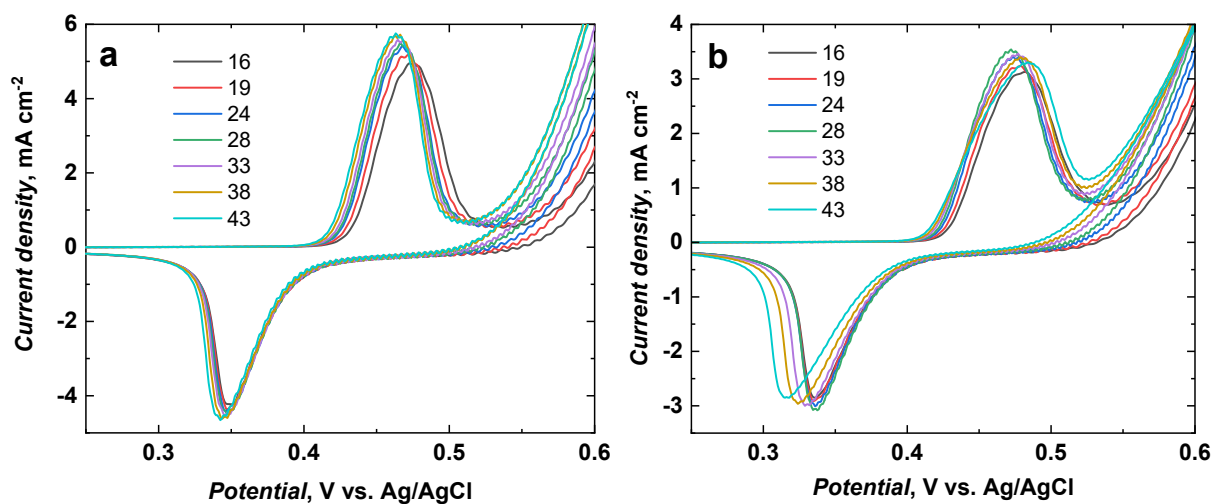
Figure S10. CV curves of (a) poly[NPs-Ni(OH)$_2$SaltMe]$_{1\,M}$ and (b) poly[*meso*-NPs-Ni(OH)$_2$SaldMe]$_{1\,M}$ performed in 1.0 M NaOH$_{aq}$ at various temperatures.

Table S1. Number of potential cycles required to generate $Ni(OH)_2$-type NPs in different $NaOH_{aq}$ concentrations.

C_{NaOHaq} (M)	Poly[NPs-Ni(OH)$_2$SaltMe]	Poly[*meso*-NPs-Ni(OH)$_2$SaldMe]
	Number of potential cycles	
0.2	120	150
0.5	100	150
1.0	130	130
2.0	130	150

Table S2. Charges of the forward and backward anodic peaks of poly[NPs-Ni(OH)$_2$SaltMe]$_{0.2\,M}$, and poly[*meso*-NPs-Ni(OH)$_2$SaldMe]$_{0.2\,M}$ measured in 0.2 M NaOH$_{aq}$.

	C_{urea} M	Poly[NPs-Ni(OH)$_2$SaltMe]$_{0.2\,M}$			Poly[*meso*-NPs-Ni(OH)$_2$SaldMe]$_{0.2\,M}$		
		Q_1 mC cm^{-2}	Q_2 mC cm^{-2}	%Q	Q_1 mC cm^{-2}	Q_2 mC cm^{-2}	%Q
Separately	0.01	10.05	5.36	53.30	28.27	17.70	62.64
	0.05	22.09	12.24	55.43	63.27	47.55	75.16
	0.1	29.95	15.77	52.64	88.52	67.24	75.97
	0.3	43.37	21.02	48.47	108.06	91.48	84.66
	0.5	44.03	21.17	48.09	126.84	87.70	69.15
Continuously	0.01	11.28	5.05	44.80	27.14	11.73	43.23
	0.05	22.40	11.53	51.48	61.02	38.01	62.29
	0.1	29.08	14.69	50.53	78.47	49.39	62.94
	0.3	43.01	20.71	48.16	109.08	76.22	69.88
	0.5	46.43	21.94	47.25	123.11	83.01	67.43

Table S3. Charges of the forward and backward anodic peaks of poly[NPs-Ni(OH)$_2$SaltMe]$_{0.5\,M}$, and poly[*meso*-NPs-Ni(OH)$_2$SaldMe]$_{0.5\,M}$ measured in 0.5 M NaOH$_{aq}$.

	C_{urea} M	Poly[NPs-Ni(OH)$_2$SaltMe]$_{0.5\,M}$			Poly[*meso*-NPs-Ni(OH)$_2$SaldMe]$_{0.5\,M}$		
		Q_1 mC cm^{-2}	Q_2 mC cm^{-2}	%Q	Q_1 mC cm^{-2}	Q_2 mC cm^{-2}	%Q
Separately	0.01	12.81	1.89	14.74	14.69	4.23	28.82
	0.05	18.16	9.13	50.28	24.69	15.56	63.02
	0.10	23.47	15.31	65.22	32.60	24.13	74.02
	0.30	39.29	33.27	84.68	51.79	42.76	82.56
	0.50	45.61	39.80	87.25	64.49	55.36	85.84
Continuously	0.01	12.91	1.84	14.23	13.52	2.60	19.25
	0.05	18.06	8.47	46.89	20.77	11.89	57.25
	0.10	22.60	14.23	62.98	28.06	19.69	70.18
	0.30	35.00	28.57	81.63	47.96	40.05	83.51
	0.50	43.57	37.50	86.07	58.16	50.36	86.58

Table S4. Charges of the forward and backward anodic peaks of poly[NPs-Ni(OH)$_2$SaltMe]$_{1\,M}$, and poly[*meso*-NPs-Ni(OH)$_2$SaldMe]$_{1\,M}$ measured in 1.0 M NaOH$_{aq}$.

	C_{urea} M	Poly[NPs-Ni(OH)$_2$SaltMe]$_{1\,M}$ Q_1 mC cm^{-2}	Q_2 mC cm^{-2}	%Q	Poly[*meso*-NPs-Ni(OH)$_2$SaldMe]$_{1\,M}$ Q_1 mC cm^{-2}	Q_2 mC cm^{-2}	%Q
Separately	0.01	13.93	7.81	56.04	10.41	5.97	57.35
	0.05	28.52	22.40	78.53	22.86	18.32	80.13
	0.1	36.84	28.67	77.84	34.03	28.16	82.76
	0.3	55.61	44.64	80.28	59.90	50.26	83.90
	0.5	66.22	54.08	81.66	74.80	63.27	84.58
Continuously	0.01	9.74	4.08	41.88	13.52	2.60	19.25
	0.05	18.52	12.91	69.70	20.77	11.89	57.25
	0.1	25.56	18.47	72.26	28.06	19.69	70.18
	0.3	41.17	30.92	75.09	47.96	40.05	83.51
	0.5	51.99	41.02	78.90	58.16	50.36	86.58

Table S5. Charges of the forward and backward anodic peaks of poly[NPs-Ni(OH)$_2$SaltMe]$_{2\,M}$, and poly[*meso*-NPs-Ni(OH)$_2$SaldMe]$_{2\,M}$ measured in 2.0 M NaOH$_{aq}$.

	C_{urea} M	Poly[NPs-Ni(OH)$_2$SaltMe]$_{2\,M}$ Q_1 mC cm^{-2}	Q_2 mC cm^{-2}	%Q	Poly[*meso*-NPs-Ni(OH)$_2$SaldMe]$_{2\,M}$ Q_1 mC cm^{-2}	Q_2 mC cm^{-2}	%Q
Separately	0.01	12.76	8.57	67.20	10.26	7.70	75.12
	0.05	35.05	36.07	102.91	28.21	28.98	102.71
	0.10	68.42	64.03	93.59	46.33	46.53	100.44
	0.30	148.47	135.46	91.24	111.79	105.77	94.61
	0.50	ND	ND	ND	171.12	130.36	76.18
Continuously	0.01	19.85	8.62	43.44	11.94	6.94	58.12
	0.05	73.78	39.49	53.53	29.34	25.20	85.91
	0.10	ND	ND	ND	47.24	38.93	82.40
	0.30	ND	ND	ND	92.96	77.81	83.70
	0.50	ND	ND	ND	113.52	98.52	86.79

ND – not determined

Table S6. The time stability of Ni(OH)$_2$ type NPs derived from poly(NiSalen)s towards urea and artificial urine.

	Poly[NPs-Ni(OH)$_2$SaltMe]$_{1\,M}$ 0.3 M urea		Poly[meso-NPs-Ni(OH)$_2$SaldMe]$_{1\,M}$ 0.3 M urea		Poly[NPs-Ni(OH)$_2$SaltMe]$_{1\,M}$ Artificial urine		Poly[meso-NPs-Ni(OH)$_2$SaldMe]$_{1\,M}$ Artificial urine	
Time	Current density	Current retention	Current density	Current retention	Current density	Current retention	Current density	Current retention
h	(mA cm^{-2})	(%)	(mA cm^{-2})	(%)	(mA cm^{-2})	(%)	(mA cm^{-2})	(%)
0.5	4.5	100.0	4.3	100.0	4.0	100.0	2.7	100.0
5	3.3	73.3	3.5	81.4	3.2	80.0	2.2	81.5
10	2.5	55.6	2.8	65.1	2.7	67.5	2.0	74.1
15	2.0	44.4	2.4	55.8	2.6	65.0	1.9	70.4